# Geoelectrical characterization of a landslide surface for investigating hazard potency, a case study in the Tehran- North freeway, Iran

Kiana Damavandi [a], Maysam Abedi [a, *], Gholam-Hossain Norouzi [a], Masoud Mojarab [a]

[a] School of Mining Engineering, College of Engineering, University of Tehran, Tehran, Iran.

## ABSTRACT

Landslide, as a geohazard issue, causes enormous threats to human lives and properties. In order to characterize the subsurface prone to the landslide which is occurred on the Tehran-North freeway, Iran, a comprehensive study focused on geological field observations, and a geoelectrical survey as a cost-effective and fast, non-invasive geophysical measurement was conducted in the area. As a result of road construction, problems in this region have increased. The Vertical Electrical Sounding (VES) investigation in the landslide area has been carried out by the Schlumberger array for data acquisition, implementing eight survey profiles varying in length between 60 and 130 m. Based on the electrical resistivity models through a smoothness-constrained least-square inversion methodology, the landslide structure (i.e., depth of the mobilized material and potential sliding surface) is better defined. The inferred lithological units, accompanied by stratigraphical data from a borehole and geological investigations for the prone landslide region, consisted of a discontinuous slip surface, having a wide range of resistivity, observed to be characterized by tuff with silt. Electrical resistivity values above 150 Ωm indicate a basement of weathered marlstone and sand. Values between 15 and 150 Ωm illustrate a shale-content layer with outcrops in the area that is the reason for movement. The sliding surface is at a depth of about 12 m. The method used in this study is a good candidate to investigate the risk of landslides in this region and can be applied to other landslide areas where borehole exploration is inefficient and expensive due to local complications.

Keywords: Vertical Electrical Sounding (VES), Geophysics, Inversion, Landslide.

## 1. Introduction

Landslide is an intricate geological phenomenon consisting of a series of layers with differing and gradational physical properties that often occur associated with road-cut slopes (shown in a schematic view in Fig. 1). This natural disaster, known as a geohazard, can be of different forms (i.e., shallow or deep-seated; rotational or translational) with active, passive, or inert conditions [1]. Landslides are caused by many factors in Iran which the utmost important reasons are the presence of rough topography, geological activities (i.e., earthquakes), meteorological conditions (i.e., heavy rainfall), destructive human activities (i.e., deforestation and industrialization), and a large amount of groundwater content [2]. However, there are few studies on landslides and their possible hazards [3,4].

A multidisciplinary methodology using the integration of satellite, airborne, ground-based sensing technologies and direct methods (e.g., laboratory tests, borehole, piezometer, and inclinometer) is often recommended to have a holistic understanding of the composition of a landslide (i.e., the depth of possible sliding surfaces, as well as the thickness and lateral extent of mobilized material). It is worth pointing out that the direct techniques yield valid parameters relating to a landslide's lithological, hydrological, and geotechnical features. These methods require labor-intensive and often costly fieldwork to achieve an accurate image of the geomechanical, not the physical properties of the rocks/soil in the subsurface, through a plethora of probes and examinations on the ground [5]. In recent times, advancements in computer processing and numerical modeling caused geophysical techniques to be more reliable as indirect, non-destructive methods in conjunction with other geotechnical investigation techniques to cover vast areas at a and low cost in the early stages of the inquiry. As a result, it is possible to be used as an option for more expensive drilling activities in some cases. Geophysical surveys fill in the holes in subsurface data and provide an enormous valuable dataset of information about the subsurface material to determine the flow of groundwater within the sliding mass and its distribution [6,7].

One of the most used techniques among geophysical surveys for subsurface characterization is geoelectrical investigations that determine the electrical resistivity distribution of the subsurface materials. Indeed, the substratum physical property described by this parameter is primarily determined by the mineralogy of the particles, porosity, the groundwater content, the composition of the electrolyte, the conductivity of pore fluid, clay content, as well as the intrinsic matrix resistivity as a function of weathering and alteration [8.9]. In contrast to electromagnetic techniques, electrical resistivity techniques are less attentive to atmospheric noise, penetrate to greater distances, are less affected by metallic artifacts and power lines, and are better at identifying resistive targets [10]. In literature, compared to ground penetrating radar [11,12] and seismic refraction/reflection methods [13,14], electrical resistivity techniques are more effective in studying the internal features of landslides. Electrical resistivity tomography is mostly appropriate for imaging unstable slopes [15,16,17,18], identifying the involved materials in the mass movement and determining the thickness and volume of a slope [19,20,21], and identification of the most likely slip surface [22,23,24].

* Corresponding author: E-mail address: maysamabedi@ut.ac.ir (M. Abedi).

The present study describes the results of a VES survey completed on a prone landslide in Iran to describe its geometry and internal structure accurately. The research site has been studied systematically and integrated with the data acquired from a borehole to learn more about the materials involved in the movement, get a better understanding of the environment of the slip surfaces, and estimate the thickness of the mobilized material.
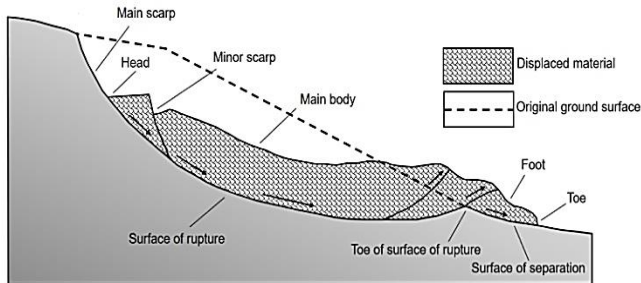


**Fig. 1.** A simple illustration of a landslide (reproduced from the work by Highland and Bobrowsky, 2008) [31].

## 2. Geological descriptions of the prone landslide area

The study area is located near the Tehran-North freeway, one of the most important communication routes in Iran between Tehran, Alborz, and the east Mazandaran provinces. The landslide region is situated in the southern part of the Central Alborz (Fig.2a) and falls within the geographical coordinates of latitude 35°58'46"N to 35°58'53"N and longitude 51°16'15"E to 51°16'30"E, approximately 20 km to the NW of Tehran city. The portion of the study area is illustrated by the white rectangle as shown in Fig. 2b, which is a landslide hazard zonation map provided by Kamranzad et al. (2016). They implemented the data-driven method in the geographic information system (GIS) environment considering six main factors in landslide occurrence, including the value of dip, dip direction, geological materials, distance from the fault, acceleration of the earthquake, and raining quantity to create the landslide hazard zonation map. The research field is a section of the Tehran map on a scale of 1:100,000 (reproduced from released maps by the Geological Survey of Iran) and is characterized by hilly terrains with surface elevation rising from 2169 m to 2258 m. In the region, the rivers and their distributaries form a dendritic drainage pattern (Fig.3a).

Tuffs and gray shale are the main outcrops of this study area (Fig.3b) which is part of the Karaj formation presenting an Eocene (lower-middle) non-homogeneous succession comprised of a relatively thick green tuff sequence, sedimentary rocks, volcanic lavas, and rarely evaporation rocks. From the drilling borehole in the landslide area, it is evident that the lithology series from bottom to top comprises weathered marlstone, alternative shale and tuff layers, and gravelly soil with silt. Also, there are conglomerate and limestone coverage verified by field observations [25].

From a tectonic viewpoint, the study area lies between two thrust faults running in the same direction as the Alborz mountain range, which means they are roughly NW-SE with 130-150 azimuth and created a system of striking sub-vertical normal faults running from the NE–SW to N–S. The presence of these faults in the vicinity of the studied landslide has caused rocks and sediments to be crushed and broken. Tectonic activities at the site of these faults have caused the expansion of joints and cracks with the instability of the mass movement and allowed water infiltration to accumulate moisture in the underlying levels, hastening the evolution of the instability. Over time, erosion and weathering have caused the mass materials to become unstable soil [26]. The studied landslide is a roto-translational type with 375 m in length, and the maximum width is 170 m (Fig. 3c).

## 3. Geoelectrical survey configuration and inversion results

Electrical resistivity tomography is a type of in-situ geophysical system combining vertical electrical sounding and resistivity profile measurement surveys. Based on the difference in electrical resistivity between the landslide material and the bedrock, it was thought to be an acceptable geophysical solution to obtain high-resolution 2D or 3D representations of the subsurface electrical resistivity distribution [27]. Note that a pseudo section is typically used to display 2D data, representing the apparent resistivity variations of the subsurface. This volumetric physical property describes the resistance of electrical current flow within an object that depends on the grain size, porosity, contents of water, and mineralization of the rocks [28].

The electrical resistivity method uses single-channel four-electrode arrays, where two steel electrodes are used to inject a regulated electric current (I) into the field and two for calculating the potential difference (V). Depending on the electrode configuration and array used, the apparent resistivity values characterizing the investigated subsoil can be determined using the described values and the geometrical coefficient (K). Multiple electrodes and a rectilinear profile with increasing inter-electrode spacing are used in electrical resistivity imaging to enable
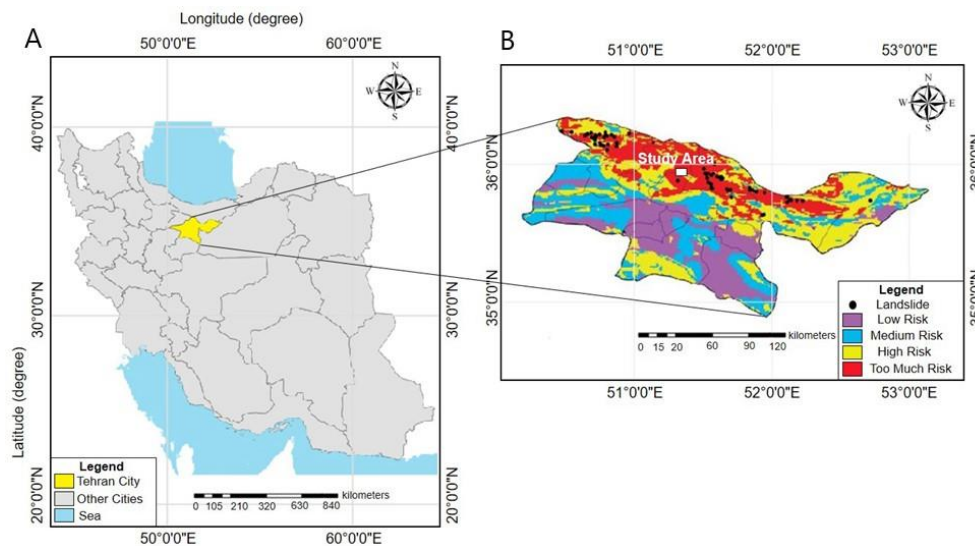


**Fig. 2.** Map of (a) Iran illustrating Tehran province in yellow, and (b) landslide hazard zonation using the data-driven method of the Tehran province [2]. A white rectangle shows the study area.
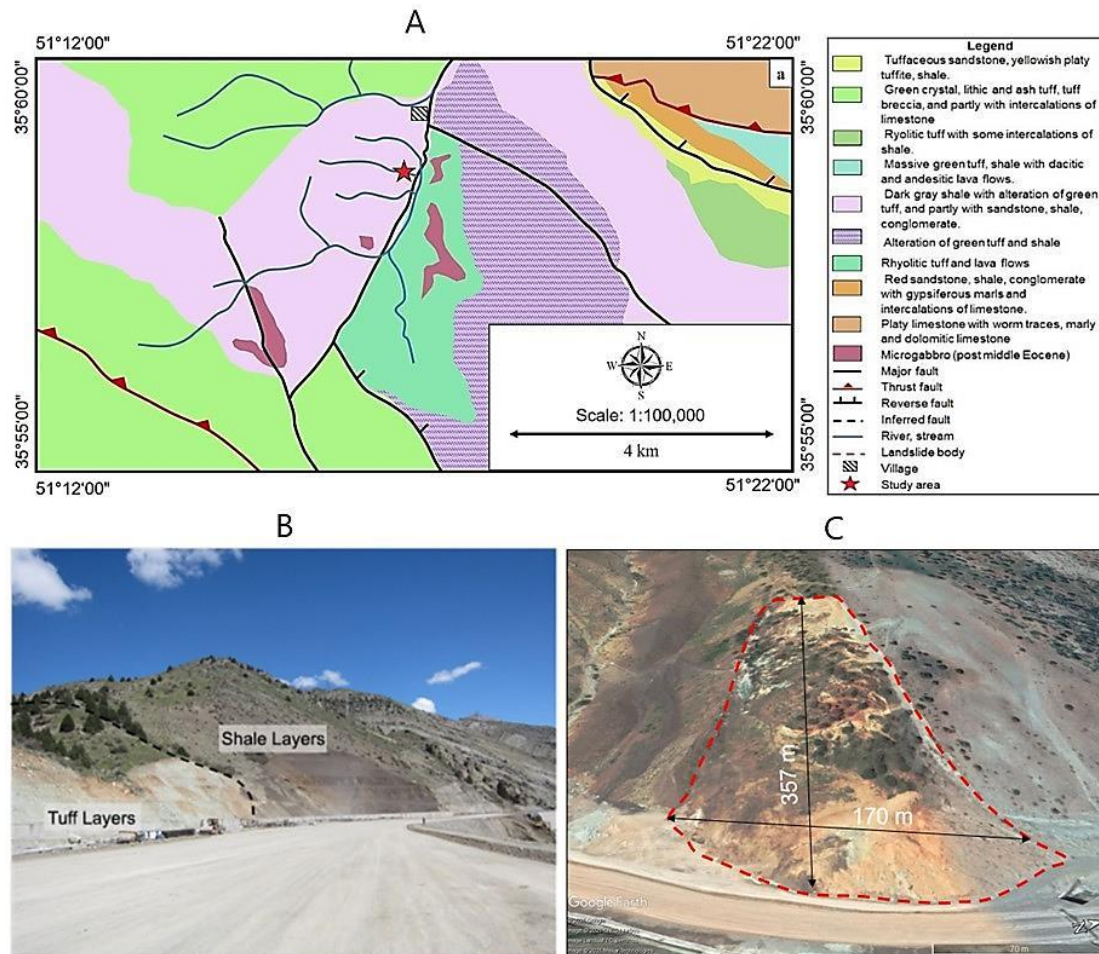
**Fig. 3.** (a) The research area's geological map. The major tectonic characteristics of the area are also depicted. (b) Presence of alternative tuff and shale layers in the vicinity of landslide area [25], (c) landslide body with its dimensions measured about 170 m in width and extends down to slope in the length of about 357 m.

different apparent resistivity values to be reported at different depths. Different depth penetration and resolution can be achieved depending on the array geometry on the display of the four electrodes, as previously stated [8].

Fig. 4a shows the 3D view of the roto-translational landslide. The geophysical investigation was applied to depict the geometry of the landslide body, estimate the thickness of sliding material, and gain a better understanding of the geological environment. The survey was conducted by deploying eight parallel electrical profiles with a line spacing of about 20 meters (except for profiles 4 and 5), varying in length from 60 to 130 m, and oriented N-S direction, based on the accessibility condition at an angle almost perpendicular to the main axis of the landslide (Fig.4b). The electrode spacing varies with the length of each profile; however, it is mostly 20 m. Apparent electrical resistivity data were collected in this study conducted by 58 electrodes, all connected to a multi-electrode system, WDDS-1, using Schlumberger array configuration, which revealed a higher signal-to-noise ratio, deeper analysis, and improved sensitivity trends to both horizontal and vertical changes in subsurface resistivity [28]. It was designed to achieve a penetrating depth of approximately 60 m. WDDS-1 is a new generation intelligence multi-electrode resistivity instrument. It can automatically measure and memorize voltage, current, apparent resistivity, and SP parameters. It is widely used in hydrological and engineering surveys, such as groundwater seeking and dam base evaluation. It also can be applied in engineering, and geological prospectings, such as metal-nonmetal mineral resources exploration, urban exploration, railway, and bridges, and even geothermal exploration. Table. 1 shows the details

of data acquisition for each station, along with eight profiles. Figure 4c presents a portion of the transverse cracks on the toe of the landslide. The sliding surface of the landslide is shale with tuff alternation and dips 30° with a dip direction of 60° in the southern part of the slide (Fig. 4d).

**Table 1.** characteristics of data acquired in the current study.

| AB/2 | MN | K |
|---|---|---|
| 3 | 2 | 12.57 |
| 5 | 2 | 37.70 |
| 7 | 2 | 75.40 |
| 10 | 5 | 58.91 |
| 15 | 5 | 137.44 |
| 20 | 5 | 247.40 |
| 30 | 5 | 561.56 |
| 40 | 5 | 1001.00 |
| 50 | 20 | 376.99 |
| 70 | 20 | 753.98 |
| 100 | 20 | 1555.00 |
| 150 | 20 | 3519.00 |
| 150 | 50 | 1374.00 |
| 200 | 50 | 2474.00 |

*AB/2 is the half distance of current electrodes, and MN is the separation distance of potential electrodes.
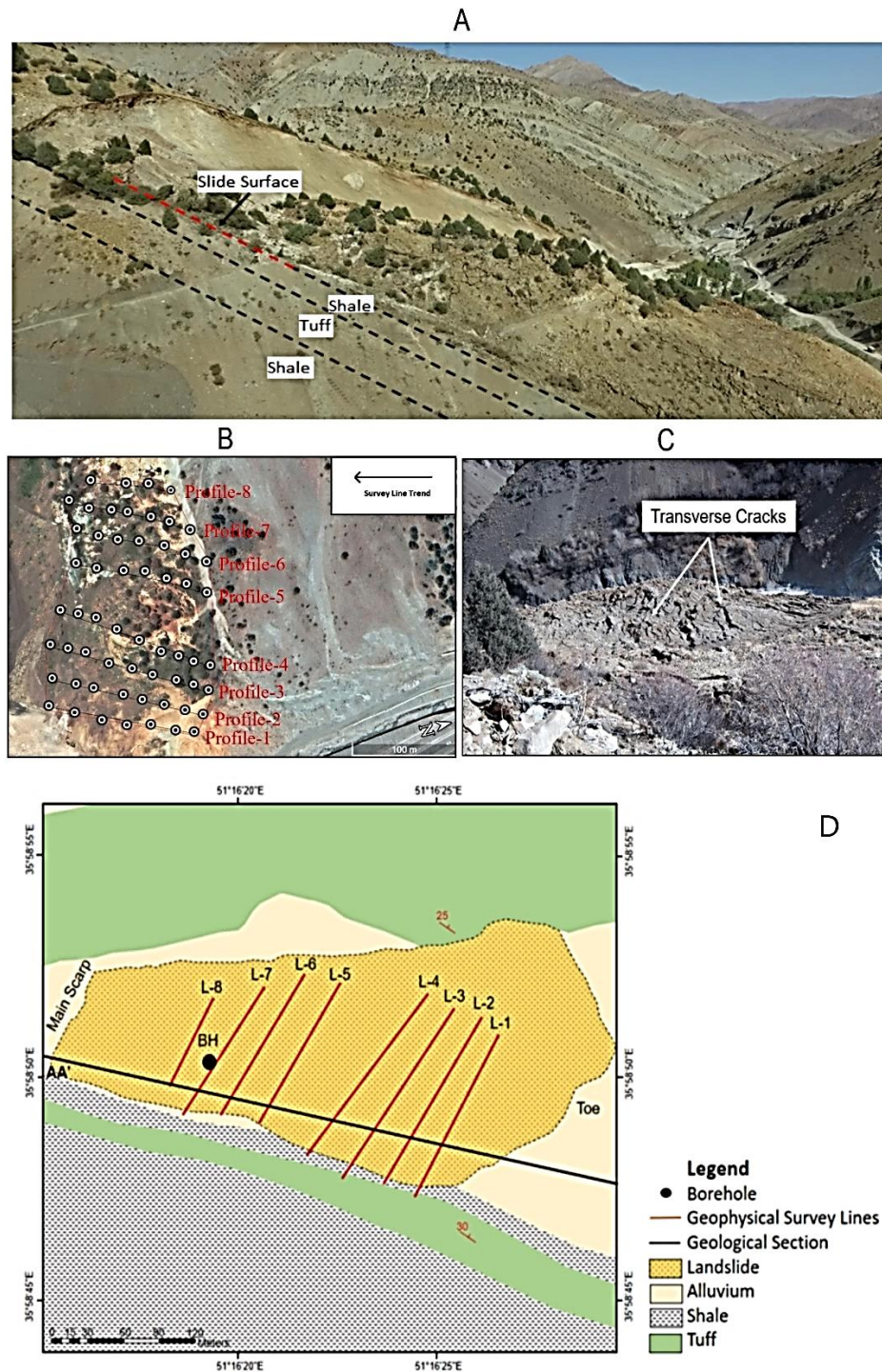
**Fig. 4.** (a) 3D view of the sliding surface. (b) plan view of data acquisition points. (c) An image of the transverse cracks near the toe of the landslide. (d) Geoelectrical profiles and location of the borehole [25].

The set of apparent resistivity values obtained from the field measurement that is raw data was later interpreted. A mathematical model with cells with varying resistivity values is created to achieve real resistivity, and recorded resistivity is inverted by a well-known and most applied software called Res2DInv. The employed code is based on a quasi-Newton optimization technique that implements a smoothness-constrained least-squares inversion which enables the computation of 2D sections using finite differences or finite elements while accounting for topographic corrections applied by providing actual electrode elevation information [29]. The aim is to generate an obvious resistivity pseudo-section that corresponds to the measured results. The inversion was carried out with a vertical to horizontal flatness filter ratio of 0.5, emphasizing horizontal subsurface structures. The root means square error (RMS) can be used to estimate the fit of the obtained resistivity model. The optimization approach changes the 2D resistivity formula, attempting to iteratively minimize the error, which indicates the percentage difference between the observed and estimated values; thus, when the error is smaller, the correspondence between the field data

and the ones of the model is greater. The inversion was carried out after 5 iterations and RMSs for profiles one to eight were 5.1%, 10.4%, 10.6%, 11.3%, 6.3%, 5.4%, 4.9%, and 6.1%, respectively. The noise level was due to measurement defects or the consequences of 3D geometry since no anthropic perturbations were apparent. Figure 5 presents the observed apparent resistivity values (Fig.5a), the calculated resistivity values (Fig.5b), and the final electrical resistivity model (Fig.5c), along with eight 2D profiles visualized in 3D.

## 4. Geoelectrical interpretation

The resistivity attribute distribution in the 2Dprofiles (from 15 to about 2500 Ωm) is very similar, showing the dependability of the inversion phase. It shows the stratigraphic sequences mainly consisting of three lithologies complemented by the information from the geological field observations and the drilling borehole of the investigated landslide (Fig.6). As a representative of the geoelectrical survey, geological interpretation along four profiles (1, 2, 4, and 5) have been presented in Fig. 7. Despite the existence of normal faults in the study area, profiles do not show any strong displacement of a resistivity body caused by faults since profiles are almost parallel to the regional fault networks. The most striking feature of profiles is the recognizable conductive shale on the middle part that separates the materials of the landslide overburden mass from the stable bedrock mass. The potential slip surface is interpreted as the vivid discontinuity in the upper part of the profiles with a depth of approximately 12 m.

The length of Profile-1 was 126 m, while that of profile 5 was 108 m. The tomography section along profile-1 and profile-2 was taken near the foot of the slide, whereas Profiles 4 and 5 were taken in the middle, covering most of the landslide. For profile 1, a shallow layer with a wide range of resistivity values coincided with the gravelly soil, which is comprised of green tuff and silt. A vast area of high resistivity (more than 150 Ωm) is equivalent to coarse-grained rocks like sandstone and marlstone. Between the depth of 12 to 60 m in profile-1, a thick conductive layer (less than 150 Ωm) is defined as a shale of the area, confirmed by field observation (Fig. 7a).

For profile-2 (Fig. 7b), a conductive layer underlying the sliding surface was observed, which may be linked to the anomalous low resistive body found in profile-1. A shallow layer coincided with the green tuff and silt, consistent with the existence of related content in section 1. It also reinforces the concentrated existence of the high-resistance (>150 m) mass, which is interpreted as a weathered layer. From Fig. 7c, profile-4 crossed with the N-S direction shows that a resistive zone of more than 150 Ωm between a depth of 12 to 50 m is known as the sandstone and marlstone. The ingredients in the shallow layer are made up of green tuff with silt and coarse-grained sediments, and the conductive area can be observed, as shown by resistivity values less than 150 Ωm interpreted as the shale level. The field survey revealed that areas with a high proportion of shale have low resistivity (<150m), for example, at depths ranging from 8 to 50 m along profile 5. The regions with a high percentage of rock blocks have high resistivity (>150 m), for example, at distances between 16 and 50 m along profile-5 (Fig. 7d). The results of the interpreted 2D data are presented as a table of values (Table 2).

In general, studying the electrical properties of a three-dimensional model must provide the most accurate results since all geological structures are three-dimensional in nature. Currently, 3D surveys are less used in geophysical studies due to their higher costs than 2D surveys. So, 2D electrical resistivity data acquired from the study area was entered into Res3DINV software for the 3D inversion process. Fig.8a shows a three-dimensional model of the apparent resistivity observed from the geophysical survey at 28 km of the Tehran-North freeway. The calculated resistivity values (Fig. 8b) show good agreement with the observed values.

Therefore, the performed algorithm has good accuracy for three-dimensional inversion. The error resulting from inversion after seven iterations are equal to 11.98%. Due to the low density of the measured data, it was expected that the obtained models would be error-prone, and only the stratification status could be deduced from them. In the inverted model (Figs. 8c and 8d), the surface layer with a wide range of resistivity values is located on the green to blue layer, which is interpreted as the shale of the area. Also, the substrate, which is considered the bedrock of the area, consists of sandstone and weathered marl, with high electrical resistivity values.
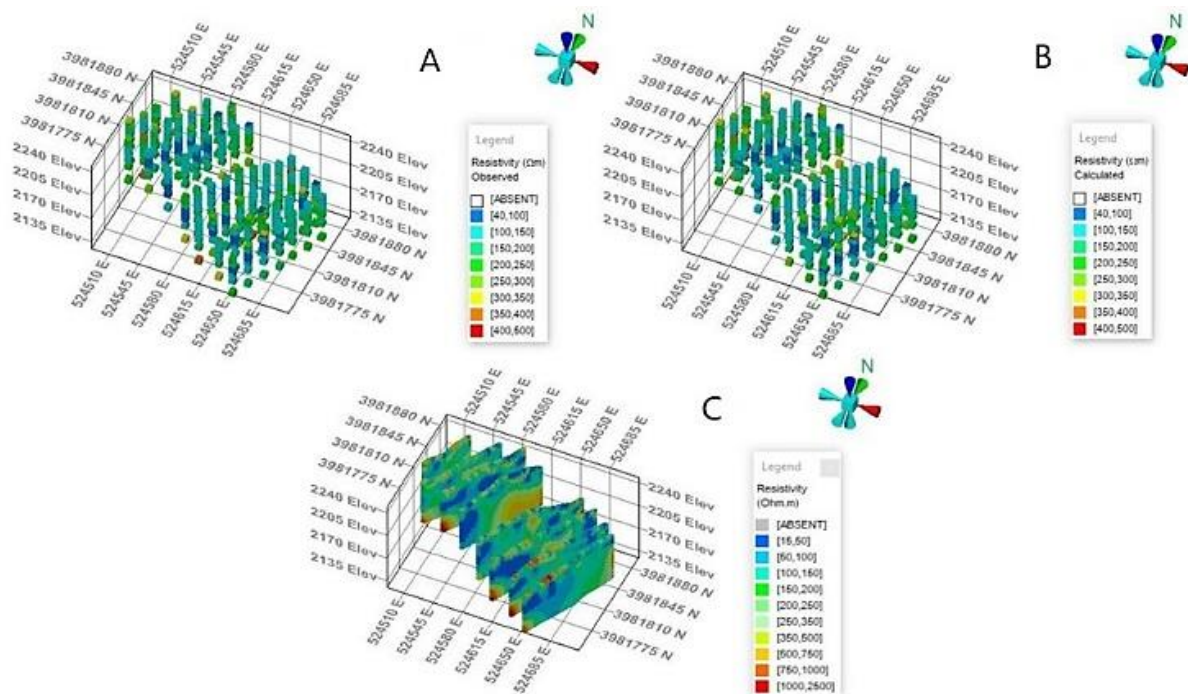


**Fig. 5.** 3D view of (a) observed apparent resistivity, (b) calculated data, and (c) inverted model.
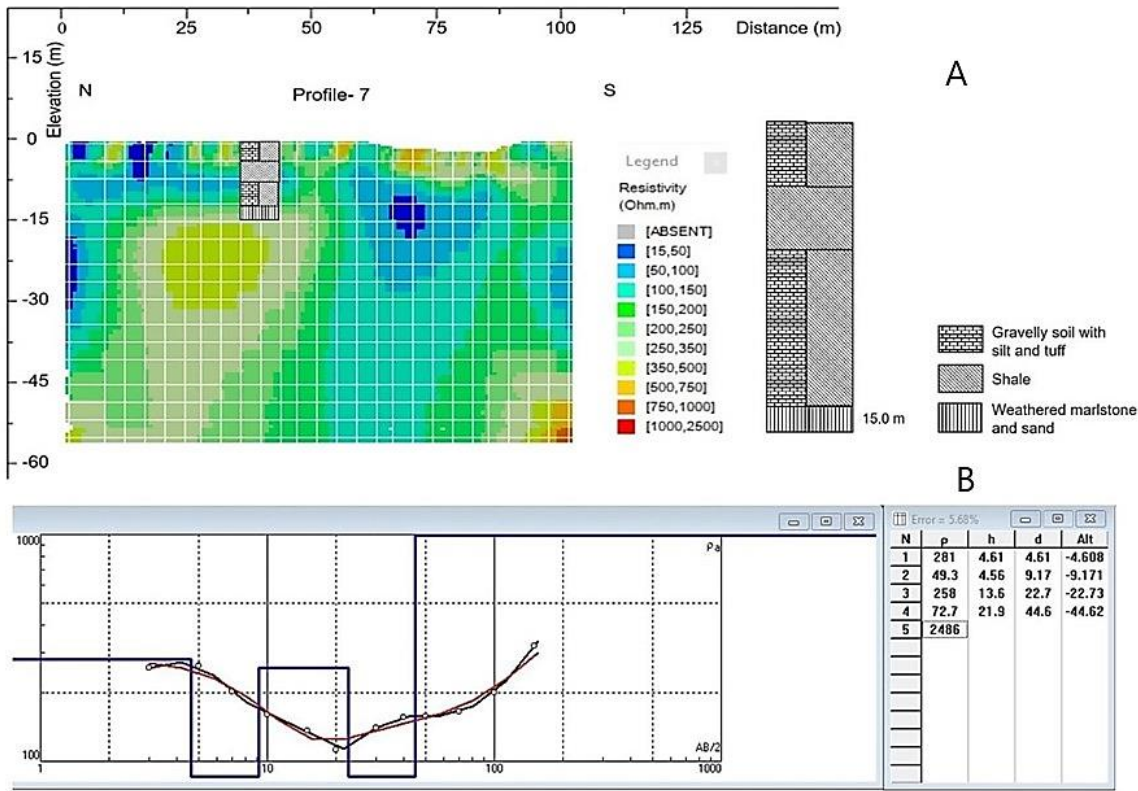
**Fig. 6.** (a) Inversion model of profile 7 accompanied by drilling borehole, (b) the sounding curve of the closest point to the borehole using IPI2WIN software.
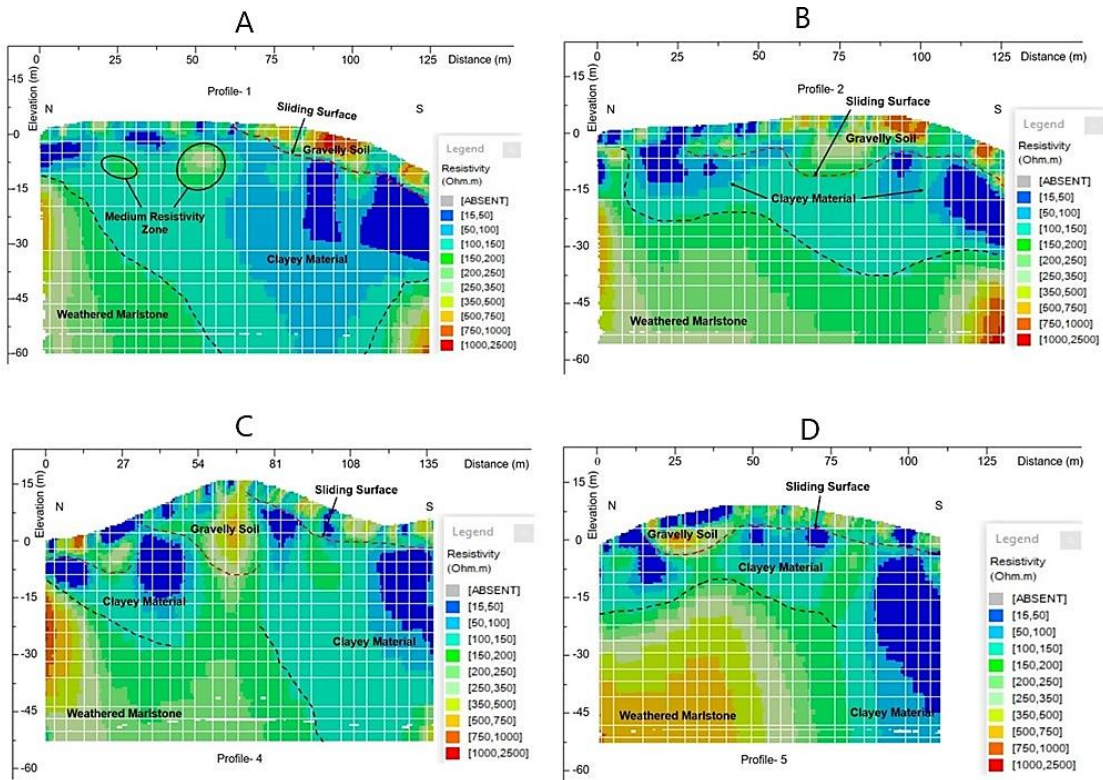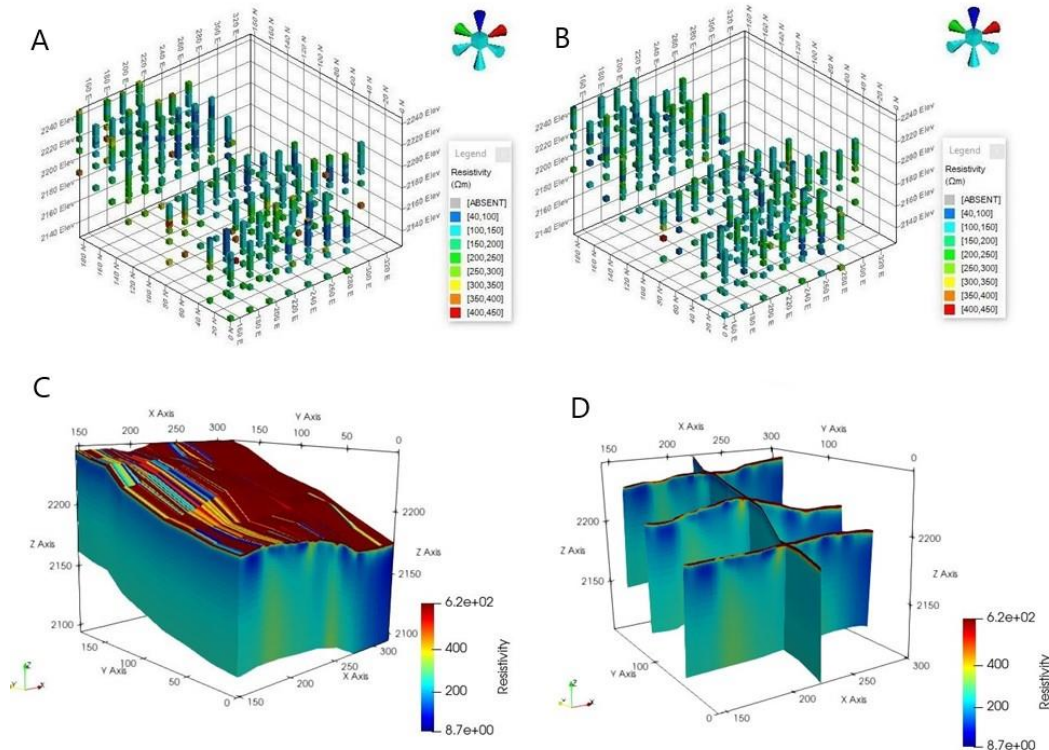


**Fig. 7.** Inversion models, (a) Profile-1, (b) Profile-2, (c) Profile-4, and (d) Profile 5.

**Table 2.** lithotypes classification based on resistivity values.

| Resistivity (Ωm) | Description | Thickness | Colour code |
|---|---|---|---|
| 15-2500 | Gravelly soil with tuff and silt | ~ 12 m | Blue-red |
| <150 | Shale | ~ 45 m | Blue- green |
| >150 | Weathered marlstone and sand | ~ 40 m | Light green- red |



**Fig. 8.** (a) observed resistivity model, (b) calculated resistivity model, (c) 3D inverted resistivity image model, (d) 3D resistivity contour plot.

The whole geophysical survey volume under investigation, as well as a 3D extraction of the geologic interpretation, is depicted in Fig.9. This figure comprises three distributions of subsurface resistivity at various depths and inferred lithology to each layer. It is possible to see conductive layers corresponding to the existence of shale superimposed over bodies with high resistivity values indicating bedrock compromised of sandstone and marlstone.

Since the whole disturbed mass has the ability to slide down the highway and obstruct it, such studies are important in many other places where cracks and scarps have formed, and knowing the probable slip surface before planning any remedial steps is necessary. The landslide in the Tehran-North highway is because of the thickness of the rubble, the nature of the slip surface, and the involvement of sandstones with fracturing areas. Potential mass motions caused by the geological composition are also possible. As a result, since the region is vulnerable to massive landslides, any effort should be made in advance to avoid such accidents. First, maintaining the equilibrium of the disrupted mass on the Tehran-North highway by planting vegetation in landslide-prone areas, according to studies and past experiences, is advised. Second, appropriate irrigation strategies must be implemented to dewater the landslide mass. Any additional water should be allowed to flow down the landslide mass into the lined drain. Third, shotcrete the surfaces of high trenches of roads. Finally, appropriate remedial measures must be taken to keep bank erosion at the toe of the landslide mass to a minimum. Basic curative steps and control systems like this would go a long way toward preventing the devastating effects of landslides and reducing the danger to life and property.

## 5. Discussion and Conclusion

Every year, landslides, the most common threat in Tehran, cause a massive loss of life and property. This high density of landslides is associated with clayey materials, heavy rainfall occurrences, erosion, and intensive urbanization. The main objective of the work was to define the thickness and characterization of mobilized material and detection of the slip surface by analyzing geophysical investigation results. The geological formations of the landslide can be well characterized utilizing the 2D survey. However, because of (1) the shallowness of the displaced materials and (2) the need to distinguish between bedrock and landslide materials, defining the landslide body remains difficult. Since resistivity is highly dependent on porosity, water content, and conductivity, this is the most important downside of geoelectrical approaches. They typically have large overlaps, preventing any direct relationship between resistivity and rock form [30].

In this research, based on the 2D data findings obtained from 58 electrical resistivity soundings with a Schlumberger array along with eight profiles, it can be mentioned that the outcropping lithotypes are represented on this site by dividing into three structures with significant electrical resistivity differences. A comparison of geographic stratigraphy and data from stratigraphic field surveys supports this view. The slipping surface structure of the area is highly resistant to changes that can be due to the presence of surface cracks, as well as alluvial materials and tuff to a depth of 12 meters. Below this structure is a layer with low resistivity (mainly less than 150 Ωm), indicating the presence of shale in the area. The presence of this layer with these characteristics
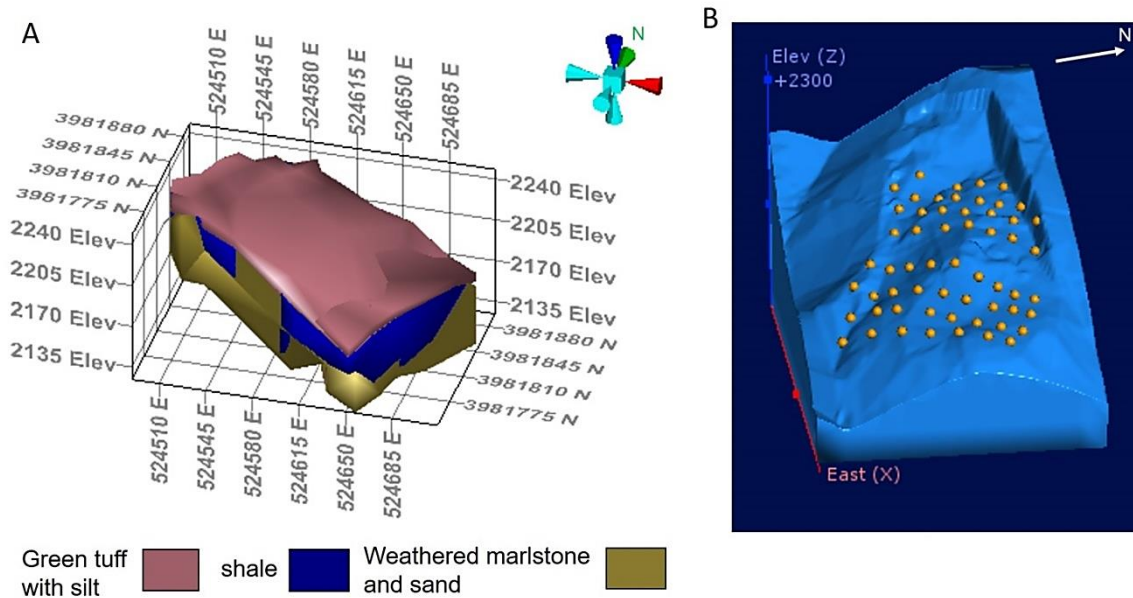
**Fig. 9.** 3D view of (a) geological map, and (b) location of 58 electrodes.

and its spread in the whole body almost uniformly can be the main cause of slipping surfaces. In the study section, in the deeper parts, below 15 meters, there is a structure with high electrical resistivity, which can be related to the presence of sandstone and marlstone. The contact surface of the two mentioned layers (tuff-alluvium and shale of the area) can slip due to the sudden change in the characteristics of each layer.

Based on the number of landslide incidents in the area over the last decade, there is a likelihood of a rise in landslide occurrence in the vicinity, particularly along the ridges where road construction is taking place. As a result, we hope to use the details presented here as a starting point for further investigation into this phenomenon, with the aim of minimizing the consequences of potential slope failures.

### Acknowledgments

### REFERENCES

[1] Fressard, M., Maquaire, O., Thiery, Y., Davidson, R., Lissak, C. (2016). Multi-method characterisation of an active landslide: Case study in the Pays d'Auge plateau (Normandy, France). Geomorphology. 270: p. 22–39. DOI: 10.1016/j.geomorph .2016.07.001.

[2] Kamranzad, F., Mohasel Afshar, E., Mojarab, M., Memarian, H. (2016). Landslide hazard zonation in Tehran province using data-driven and AHP methods. Geoscience. 25 (97): p. 101–114.

[3] Ehteshami-Moinabadi, M., Nasiri, S. (2019). Geometrical and structural setting of landslide dams of the Central Alborz: a link between earthquakes and landslide damming. Bull. Eng. Geol. Environ. 78 (1): p. 69–88. DOI: 10.1007/s10064-017-1021-8.

[4] Rezaei, S., Shooshpasha, I., Rezaei, H. (2019). Reconstruction of landslide model from ERT, geotechnical, and field data, Nargeschal landslide, Iran. Bull. Eng. Geol. Environ. 78 (5): p. 3223–3237. DOI: 10.1007/s10064-018-1352-0.

[5] Samodra, G., Ramadhan, M.F., Sartohadi, J., Setiawan, M.A., Christanto, N., Sukmawijaya, A. (2020). Characterization of displacement and internal structure of landslides from multitemporal UAV and ERT imaging. Landslides, 17 (10): p. 2455–2468. DOI: 10.1007/s10346-020-01428-0.

[6] Yılmaz, S., Narman, C. (2015). 2-D electrical resistivity imaging for investigating an active landslide along a ridgeway in Burdur region, southern Turkey. Arab. J. Geosci. 8 (5): p. 3343–3349. DOI: 10.1007/s12517-014-1412-0.

[7] Ling, C., Xu, Q., Zhang, Q., Ran, J., Lv, H. (2016). Application of electrical resistivity tomography for investigating the internal structure of a translational landslide and characterizing its groundwater circulation (Kualiangzi landslide, Southwest China). J. Appl. Geophys. 131: p. 154–162. doi: 10.1016/j.jappgeo.2016.06.003.

[8] Perrone, A., Lapenna, V., Piscitelli, S. (2014). Electrical resistivity tomography technique for landslide investigation: A review. Earth-Science Rev. 135: p. 65–82. doi: 10.1016/j.earscirev.2014.04.002.

[9] Supper, R., Ottowitz, D., Jochum, B., Kim, J.H., Romer, A., Baron, I., Pfeiler, S., Lovisolo, M., Gruber, S., Vecchiotti, F. (2014). Geoelectrical monitoring: An innovative method to supplement landslide surveillance and early warning. Near Surf. Geophys. 12 (1): p. 133–150. DOI: 10.3997/1873-0604.2013060.

[10] Blome, M., Maurer, H., Greenhalgh, S. (2011). Geoelectric experimental design - Efficient acquisition and exploitation of complete pole-bipole data sets. Geophysics. 76 (1). DOI: 10.1190/1.3511350.

[11] Carpentier, S., Konz, M., Fischer, R., Anagnostopoulos, G., Meusburger, K., Schoeck, K. (2012). Geophysical imaging of shallow subsurface topography and its implication for shallow landslide susceptibility in the Urseren Valley, Switzerland. J. Appl. Geophys. 83: p. 46–56. doi: 10.1016/j.jappgeo.2012.05.001.

[12] Kannaujiya, S., Chattoraj, S.L., Jayalath, D., Champati ray, P.K., Bajaj, K., Podali, S., Bisht, M.P.S. (2019). Integration of satellite remote sensing and geophysical techniques (electrical resistivity tomography and ground penetrating radar) for landslide

characterization at Kunjethi (Kalimath), Garhwal Himalaya, India. Nat. Hazards. 97 (3): p. 1191–1208. DOI: 10.1007/s11069-019-03695-0.

[13] Malehmir, A., Bastani, M., Krawczyk, C.M., Gurk. M., Ismail, N., Polom, U., Persson, L. (2013). Geophysical assessment and geotechnical investigation of quick-clay landslides - A Swedish case study. Near Surf. Geophys. 11 (3): p. 341–350. DOI: 10.3997/1873-0604.2013010.

[14] Imani, P., Tian, G., Hadiloo, S., El-raouf, A.A. (2020). Application of combined electrical resistivity tomography (ERT) and seismic refraction tomography (SRT) methods to investigate Xiaoshan District landslide site: Hangzhou, China. Appl. Geophys. 184.

[15] Meric, O., Garambois, S., Jongmans, D., Wathelet, M., Chatelain, J.L., Vengeon, J.M. (2005). Application of geophysical methods for the investigation of the large gravitational mass movement of Séchilienne, France. Can. Geotech. J. 42 (4): p. 1105–1115. DOI: 10.1139/t05-034.

[16] Rønning, J.S., Ganerød, G.V., Dalsegg, E., Reiser, F. (2014). Resistivity mapping as a tool for identification and characterisation of weakness zones in crystalline bedrock: definition and testing of an interpretational model. Bull. Eng. Geol. Environ. 73 (4): p. 1225–1244. DOI: 10.1007/s10064-013-0555-7.

[17] Solberg, I.L., Hansen, L., Rønning, J.S., Haugen, E.D., Dalsegg, E., Tønnesen, J.F. (2012). Combined geophysical and geotechnical approach to ground investigations and hazard zonation of a quick clay area, mid Norway. Bull. Eng. Geol. Environ. 71 (1): p. 119–133. doi: 10.1007/s10064-011-0363-x.

[18] Mita, M., Glazer, M., Kaczmarzyk, R., Dąbrowski, M., Mita, K. (2018). Case study of electrical resistivity tomography measurements used in landslides investigation, Southern Poland. Contemp. Trends Geosci. 7 (1): p. 110–126. DOI: 10.2478/ctg-2018-0007.

[19] de Bari, C., Lapenna, V., Perrone, A., Puglisi, C., Sdao, F. (2011). Digital photogrammetric analysis and electrical resistivity tomography for investigating the Picerno landslide (Basilicata region, southern Italy). Geomorphology. 133:34–46. doi.org/10.1016/j.geomorph.2011.06.013

[20] Viero, A., Galgaro, A., Morelli, G., Breda, A., Francese, R.G. (2015). Investigations on the structural setting of a landslide-prone slope by means of three-dimensional electrical resistivity tomography. Nat. Hazards. 78 (2): p. 1369–1385. DOI: 10.1007/s11069-015-1777-8.

[21] Falae, P.O., Kanungo, D.P., Chauhan, P.K.S., Dash, R.K. (2019). Electrical resistivity tomography (ERT) based subsurface characterisation of Pakhi Landslide, Garhwal Himalayas, India. Environ. Earth Sci. 78 (14). DOI: 10.1007/s12665-019-8430-x.

[22] Lapenna, V., Lorenzo, P., Perrone, A., Piscitelli, S., Rizzo, E., Sdao, F. (2005). 2D electrical resistivity imaging of some complex landslides in the Lucanian Apennine chain, southern Italy. Geophysics. 70 (3): p. 11–18. DOI: 10.1190/1.1926571.

[23] Bellanova, J., Calamita, G., Giocoli, A., Luongo, R., Macchiato, M., Perrone, A., Uhlemann, S., Piscitelli, S. (2018). Electrical resistivity imaging for the characterization of the Montaguto landslide (southern Italy). Eng Geol. 243:272–281. https://doi.org/10.1016/j.enggeo.2018.07.014

[24] Jianjun, G., Zhang, Y.X., Xiao, L. (2020). An application of the high-density electrical resistivity method for detecting slide zones in deep-seated landslides in limestone areas. J. Appl. Geophys. 177. DOI: 10.1016/j.jappgeo.2020.104013.

[25] BZP consult engineers. (2018). Engineering geology, sustainability analysis, and presenting sliding trench safety solutions in the area of 28 km of Tehran- North freeway.

[26] Yassaghi, A., Abassi, A.R. (2005). Geometry and kinematic analysis of Laniz structural sub-zone; evidence for structural evlution of south central Alborz. Geoscience. 56: p. 152–167.

[27] Bichler, A., Bobrowsky, P., Best, M., Douma, M., Hunter. J., Calvert, T., Burns, R. (2004). Three-dimensional mapping of a landslide using a multi-geophysical approach: The Quesnel Forks landslide. Landslides. 1(1): p. 29–40. DOI: 10.1007/s10346-003-0008-7.

[28] Loke, M.H. (2015). Tutorial: 2D and 3D electrical imaging surveys.

[29] Barker, R.D., Loke, M.H. (1996) Practical techniques for 3D resistivity surveys and data inversion. Geophys. Prospect. 44 (3): p. 499–523.

[30] Reynolds, J.M. (1997). An introduction to applied and environmental geophysics. An Introd. to Appl. Environ. Geophys. DOI: 10.1071/pvv2011n155.

[31] Highland, L.M., Bobrowsky, P. (2008). The landslide Handbook A guide to understanding landslides. US Geol. Surv. Circ. 1325: p. 1–147, 2008, DOI: 10.3133/cir1325.